

Corrosion Mechanisms of Mild Steel in the Presence of Formic Acid and Acetic Acid

Sahithi Ayyagari, Maryam Eslami, Bruce Brown, Srdjan Nesic
Institute for Corrosion and Multiphase Technology, Ohio University
342 W State Street
Athens, Ohio, 45701
USA

ABSTRACT

The presence of organic acids such as formic acid, acetic acid and propionic acid in oil field brines has been identified as a significant contributor to corrosion of mild steel. Extensive research indicates that corrosion rates of steel are significantly higher in weak acid environments, such as aqueous CO₂ or acetic acid, as opposed to fully dissociated aqueous strong acids at the same pH. A general observation is that the increase in corrosion rate is due to increase in cathodic current, which is due to the partial dissociation of the weak acid. Most corrosion research with respect to aqueous organic acid environments has focused on acetic acid as it is a prevalent organic acid found in oil fields; it is also a good representative for higher molecular weight carboxylic acids with similar acid dissociation constants (K_a) values that may be present, e.g., propionic acid. However, the difference in acidity of formic acid as compared to acetic acid emphasizes the need to establish a mechanistic understanding of the role of operational parameters such as pH, temperature, and/or concentration of undissociated acid concentrations on corrosion behavior. A conventional three electrode glass cell equipped with a rotating disc electrode was used to conduct electrochemical measurements (potentiodynamic sweeps, electrochemical impedance spectroscopy, and linear polarization resistance) on an API 5L X65 steel working electrode in a 1 wt.% NaCl electrolyte maintained at constant pH and temperature. It was confirmed that both formic acid and acetic acid have a similar effect on the cathodic reaction rate, wherein their contribution to the corrosion process is through chemical dissociation, which induces the buffering effect. However, while acetic acid has a slight inhibitive effect on the anodic reaction rate, a similar effect was not observed in the presence of formic acid. The effects of concentration of undissociated acid, temperature, pH, rotational speed, and presence of CO₂ in the environment on corrosion of mild steel were established.

Key words: Organic acid, acetic acid, formic acid, corrosion, electrochemical measurements

INTRODUCTION

Corrosion is a surface phenomenon, which is defined as the deterioration of a material due to chemical and/ or electrochemical reactions. The continued interest in understanding corrosion phenomena and devising mitigation methods stems from the potential influence corrosion has on infrastructural damage across diverse industries. The most prevalent forms of corrosion encountered in the oil and gas industry are referred to as sweet and sour, corresponding to aqueous CO₂ and H₂S environments, respectively. The presence of an aqueous phase in these environments leads to the formation of a weak acid which is understood to be detrimental to the service life of carbon steel pipelines, when not properly mitigated.

Corrosion rates of steel have been recorded to be notably higher in weak acid environments as opposed to fully dissociated aqueous strong acids at the same pH.¹ A general observation is that the increase in corrosion rate is due to an increase in cathodic current, which is due to the partial dissociation of the weak acid.² Volatile organic acids such as formic acid, acetic acid, and propionic acid are generally present in oil field conditions, which increase the corrosivity of the sweet and sour environments.³ Acetic acid is one of the most prevalent organic compounds found in oil fields and is considered as representative of carboxylic acids when it comes to corrosion research.⁴ Concentrations of acetic acid up to thousands of ppm have been reportedly measured,⁵ and an increase in the corrosion rate of carbon steel has been observed with acetic acid concentrations as low as 1 mM.⁶

In order to investigate the role of acetic acid on the corrosion mechanisms of mild steel, Kahyarian⁷ implemented an improved experimental procedure using a Rotating Disk Electrode (RDE) glass cell setup, which has a laminar flow profile even at a rotational speed of 2000 rpm. The adopted experimental procedure ensured that the cathodic reaction remained under charge transfer control in the set operating conditions. His research concluded that the direct reduction of acetic acid is insignificant and the increase in cathodic current is a result of the “buffering effect”.⁷ As per this mechanism, while hydrogen reduction remains to be the dominant cathodic reaction, chemical dissociation of the weak acid replenishes the hydrogen ions that are consumed during the corrosion process. Corrosion mechanisms of mild steel in other environments such as CO₂, H₂S, etc., were explained using similar theory because of the similarity in the chemical dissociation properties of weak acids.

While most of the available literature is largely focused on acetic acid because of its predominance in oil fields, the fact that formic acid has a significantly lower pKa (negative base-10 logarithm of Ka) value (stronger acid) as compared to other carboxylic acids indicates that it cannot be grouped under the umbrella of ‘Acetic Acid Research’ and accentuates the need to study its effect separately (Figure 1).

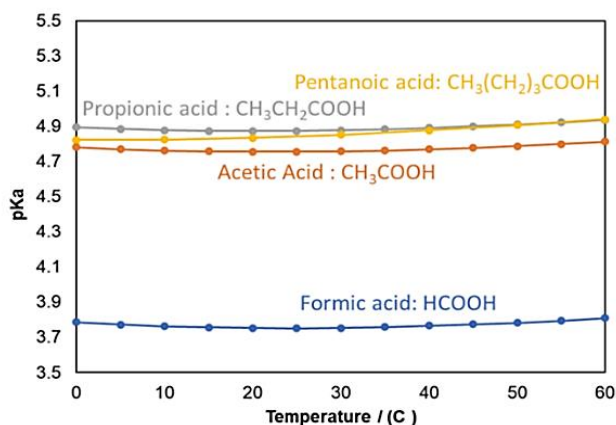


Figure 1: Dissociation constants of organic acids commonly found in oil fields ^{8,9}

The purpose of this study is to determine the effect of formic acid on corrosion mechanisms to aid in the prediction of corrosion rates of mild steel in upstream oil and gas environments. To achieve this objective,

targeted experiments over an extended range of operating conditions, at different pH, temperatures, concentrations, rotation speeds, and environments were conducted to establish the effect of each parameter on the corrosion mechanism of mild steel in the presence of formic acid. Further, the corrosion mechanisms of mild steel in the presence of formic acid and acetic acid were compared under selected operating conditions.

EXPERIMENTAL

Equipment

A 2-liter three-electrode glass cell equipped with a rotating disc electrode was used in this study. Electrochemical measurements were conducted in a 1wt% NaCl solution at a rotational speed of 2000 rpm in N₂/CO₂ sparged environments at a constant bulk solution pH. API X65 steel was used as the working electrode material for the current study. Table 1 shows the chemical composition of the working electrode.

Table 1
Chemical composition of the mild steel material (API 5L X65) (in wt.%)

Al	As	C	Co	Cr	Cu	Mn	Mo	Nb	Ni
0.028	0.008	0.05	<0.001	0.252	0.173	1.51	0.092	0.034	0.291
P	S	Sb	Si	Sn	Ti	V	Zr	Fe	
0.004	<0.001	<0.001	0.167	0.002	0.012	0.04	<0.001	balance	

Figure 2 shows the different parts of the experimental setup. An Ag/AgCl electrode was used as the reference, while a platinum mesh was used as the counter electrode. The working electrodes were 5mm diameter disks press fit into Teflon sample holders. The working electrodes were metallographically polished using 600, 800, 1000 and 1200 grit SiC abrasive papers, followed by diamond polishing using 9, 3, and 0.25µm diamond suspensions.

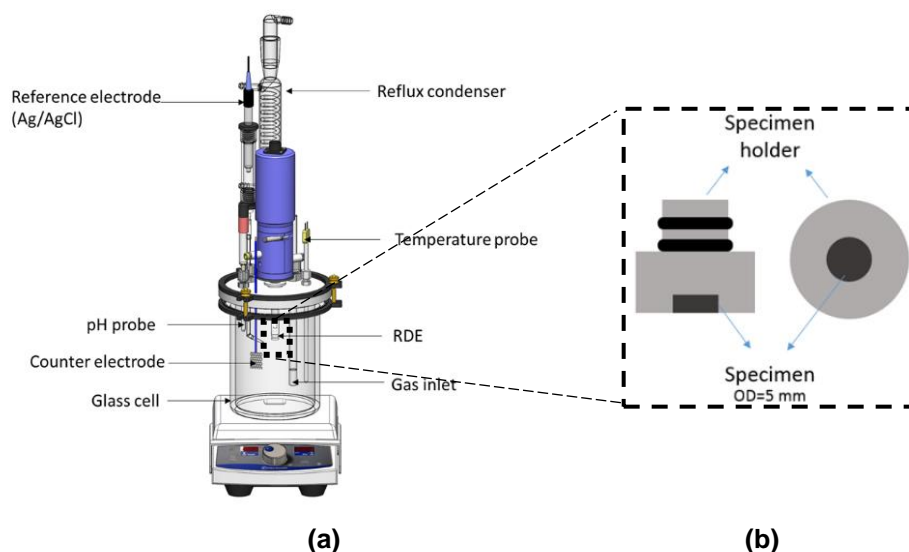


Figure 2: Experimental setup showing (a) glass cell with RDE as working electrode (b) 5mm disk press fit into a Teflon holder.

Test Matrix

The electrochemical experiments were conducted in the presence of organic acids in a 1 wt% NaCl solution de-aerated for 2h with N₂ or CO₂ sparging. The solution was continuously sparged with N₂ or

CO₂ throughout the duration of the experiment. The temperature (30°C, 50°C, or 80°C) and pH (4, 5, or 6) of the test solution were monitored and held constant. The range of experimental parameters used in the current study are shown in Table 2. The test matrices for each experimental set are detailed in the discussion section.

Table 2
Superset of experimental parameters used in the present study

Parameter	Description	
Electrolyte	1 wt% NaCl	
RDE rotation speed (rpm)	1000 – 4000	
Organic Acid (total) (mM)	HAc [†] (0 – 16.67)	HFr [‡] (0 – 39.14)
Organic Acid (total) (ppm)	HAc (0 – 1000)	HFr (0 – 1800)
Fixed pH	4.00 – 6.00 (± 0.02)	
Temperature (°C)	30 – 80 (± 2)	
Sparge gas	N ₂ or CO ₂	

Electrochemical measurements

The electrochemical measurements were performed using Gamry[§] Potentiostat and conducted twice for each experimental condition. Each experiment consisted of 5 electrochemical tests in specific order: open circuit potential (OCP) + electrochemical cleaning (30 min), OCP + cathodic sweep (55 min), OCP + electrochemical impedance spectroscopy (EIS) (40 min), OCP + linear polarization resistance (LPR) (5 min), and finally OCP + anodic sweep (25 min). An electrochemical cleaning procedure was performed on the working electrode to ensure repeatability of results. This was performed by pulsing currents (± 5 A/m², ± 2 A/m², and ± 1 A/m² in that order) for 60s at each current, followed by 120s at open circuit potential (OCP), i.e., + 5 A/m² for 60s, followed by -5 A/m² for 60s, followed by 120s at OCP, then repeat the procedure for +2 A/m², etc. After electrochemical cleaning, the OCP was monitored for 20 min until a steady state value was obtained. This was followed by cathodic polarization, EIS, LPR, and anodic polarization, as defined in Table 3. The total duration of each experiment was 4.5 h (2h of de-aeration, sample insertion and 2.5h of electrochemical tests).

Table 3
Parameters for electrochemical measurements

Technique	Parameters	Results
Potentiodynamic Sweeps	Scan Rate: 0.5 mV / s, Sampling period: 1s Cathodic: 0 to -0.55 V (vs. OCP), Anodic: 0 to 0.15 V (vs. OCP)	Mechanisms
Linear Polarization Resistance	Scan Rate: 0.125 mV / s. Polarization range: ± 5 mV (vs. OCP).	Polarization resistance (Rp)
Electrochemical Impedance Spectroscopy	Frequency range: 10000 Hz ~ 0.1 Hz. Amplitude: 10 mV. DC Potential: 0 vs. OCP	Solution resistance (Rs)

[†] Acetic acid may also be written as its shorthand chemical formula, HAc.

[‡] Formic acid may also be written as its shorthand chemical formula, HFr.

[§] Trade name

RESULTS

Corrosion mechanisms of mild steel in the presence of formic acid

Electrochemical tests were performed to see the effect of different parameters on the anodic and cathodic mechanisms. Table 4 shows the detailed operational parameters used for each test series. For each of the test series, anodic and cathodic polarization curves were obtained, and these results were corrected for IR drop using R_s obtained from EIS measurements. Corrosion rates were calculated using R_p obtained from LPR, R_s obtained from EIS measurements, and B values of 13.2 mV/dec for tests conducted at 30 °C, 14 mV/dec at 50 °C, and 15.5 mV/dec at 80 °C.

Table 4
Parameters for experiments conducted in N₂ sparged solution

Parameter	HFr concentration				Effect of pH			Effect of rotational speed			Effect of temperature		
	0	0.39	3.91	39.14	3.91	26.38	251.1	1000	2000	4000	3.91	3.82	3.41
Electrolyte	1 wt% NaCl				1 wt% NaCl			1 wt% NaCl			1 wt% NaCl		
RDE rotation speed (rpm)	2000				2000			1000	2000	4000	2000		
Total HFr (mM)	0	0.39	3.91	39.14	3.91	26.38	251.1	3.91			3.91	3.82	3.41
Undissociated HFr (mM)	0	0.14	1.41	14.18	1.41			1.41			1.41		
pH	4.00 ± 0.02				4	5	6	4.00 ± 0.02			4.00 ± 0.02		
Temperature(°C)	30 ± 2				30 ± 2			30 ± 2			30	50	80
Spurge gas	N ₂				N ₂			N ₂			N ₂		

Effect of different undissociated HFr concentrations on corrosion

Figure 3 shows potentiodynamic sweeps of X65 steel in N₂ sparged environment with different concentrations of undissociated HFr in the solution. While there is an increase in the limiting currents with increasing concentration of HFr, the charge transfer part of the cathodic polarization curve remains uninfluenced. This is a clear indication that the hydrogen evolution reaction is the main cathodic reaction and HFr influences the corrosion rate by the “buffering effect”. These results confirm that HFr is not electroactive. HFr is a strong buffer that readily dissociates when needed. It can also be observed that the anodic reaction rates are not significantly influenced by the increase in concentration of HFr.

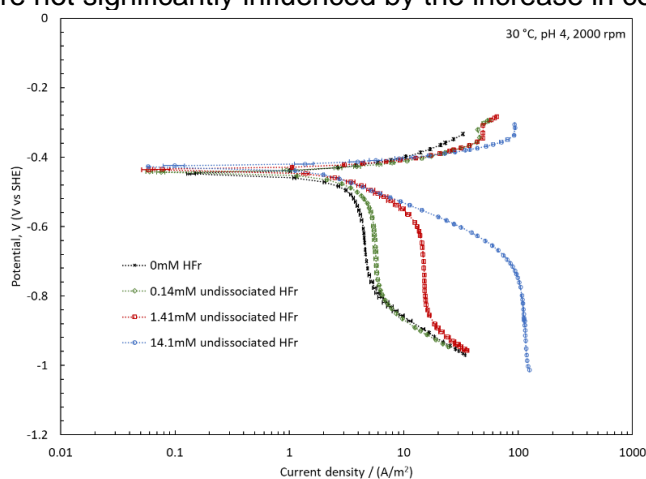


Figure 3: Polarization curves for X65 steel RDE in various concentrations of HFr at pH 4, 2000 rpm, 30°C in N₂ sparged 1 wt% NaCl solution.

© 2022 Association for Materials Protection and Performance (AMPP). All rights reserved. No part of this publication may be reproduced, stored in a retrieval system, or transmitted, in any form or by any means (electronic, mechanical, photocopying, recording, or otherwise) without the prior written permission of AMPP.

Positions and opinions advanced in this work are those of the author(s) and not necessarily those of AMPP. Responsibility for the content of the work lies solely with the author(s).

As the corrosion mechanism is primarily under charge transfer control, the increase in concentration of undissociated HFr does not significantly increase the corrosion rate. The corrosion rates in different concentrations of HFr are shown in Figure 4.

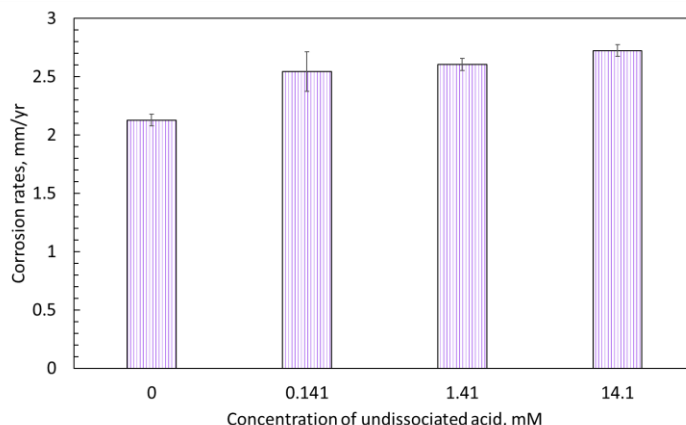


Figure 4: Comparison of corrosion rates of X65 steel RDE in various concentrations of HFr at pH 4, 2000 rpm, 30°C in N₂ sparged 1 wt% NaCl solution.

Effect of pH on corrosion in the presence of HFr

Figure 5 shows the effect of pH on corrosion behavior of steel in the presence of 1.41 mM of undissociated HFr. As pH increases, the concentration of hydrogen ions in the system decreases. This results in a significant decrease in the cathodic reaction rate as can be seen in the polarization curves. A significant increase in the anodic reaction rate with increase in pH is also observed. A similar observation was reported in the literature.¹⁰ An accurate understanding of the effect of pH on anodic reaction rate and reaction mechanism in the presence of HFr species requires comprehensive investigation, which will be part of a future study.

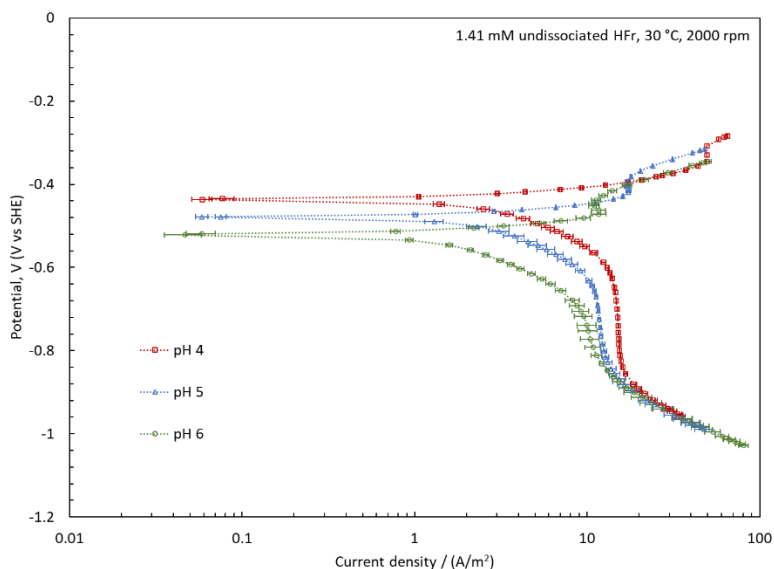


Figure 5: Polarization curves for X65 steel RDE in N₂ sparged environment at 30°C, 2000 rpm, 1.41 mM undissociated HFr at pH 4, 5, & 6.

The enhanced anodic reaction rate and the receded cathodic reaction rate with an increase in pH results in a decrease in the corrosion rates as shown in Figure 6.

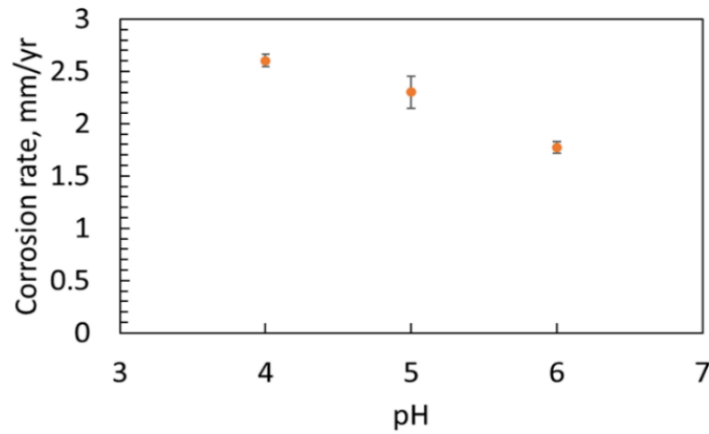


Figure 6: Corrosion rates of X65 steel RDE in N₂ sparged environment at 30°C, 2000 rpm, 1.41 mM undissociated HFr at pH 4, 5, & 6.

Effect of rotational speed of RDE on corrosion in the presence of HFr

Figure 7 shows the effect of RDE rotational speed on corrosion behavior of X65 steel in the presence of 1.41 mM of undissociated HFr. With an increase in rotational speed of RDE from 1000 rpm to 4000 rpm, there is a clear increase in the limiting current region of the cathodic curve. Despite this effect, there was no significant change in the corrosion rates in these conditions confirming that the reaction is mostly under charge transfer control. **Figure 8** shows the corrosion rates for each rotational speed.

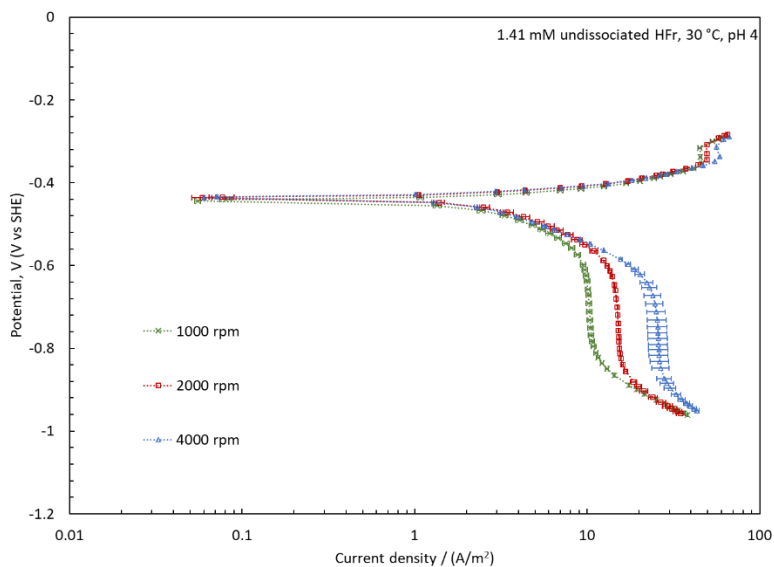


Figure 7: Polarization curves for X65 steel RDE in N₂ sparged environment at 30°C, pH 4, 1.41 mM undissociated HFr at 1000, 2000, & 4000 rpm.

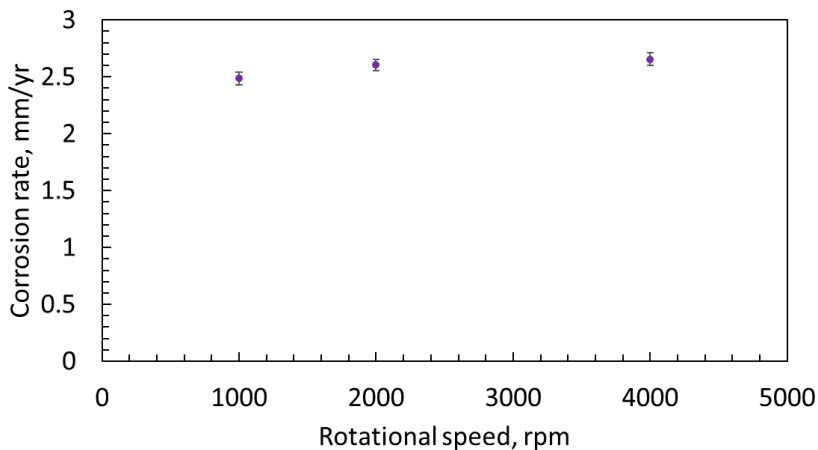


Figure 8: Corrosion rates of X65 steel RDE in N_2 sparged environment at 30°C, pH 4, 1.41 mM undissociated HFr at 1000, 2000, & 4000 rpm.

Effect of temperature on corrosion in the presence of HFr

Figure 9 illustrates the effect of temperature on corrosion behaviour of steel in the presence of 1.41 mM of undissociated HFr. The anodic curve and the charge-transfer part of the cathodic curve represent Arrhenius type reactions that are directly influenced by temperature. Additionally, temperature leads to an increase in the rate of chemical dissociation of HFr and aids in the mass transfer of species. Therefore, as temperature increases, there is an overall increase in the anodic and cathodic reaction rates. The reaction changes from a mostly charge transfer controlled mechanism to a mostly mass transfer-controlled mechanism. The accelerated reaction rates lead to an increase in the corrosion rates shown in Figure 10.

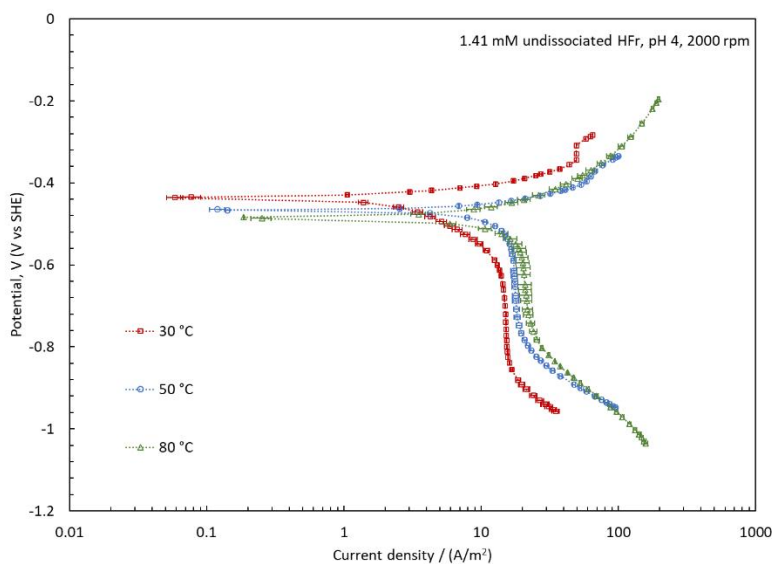


Figure 9: Polarization curves for X65 steel RDE in N_2 sparged environment at pH 4, 2000 rpm, 1.41 mM undissociated HFr at 30, 50, & 80°C.

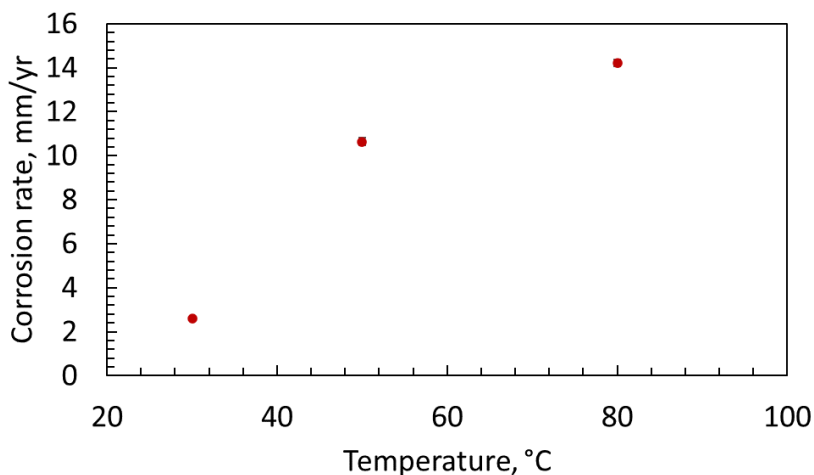


Figure 10: Corrosion rates of X65 steel RDE in N₂ sparged environment at pH 4, 2000 rpm, 1.41 mM undissociated HFr at 30, 50, & 80°C.

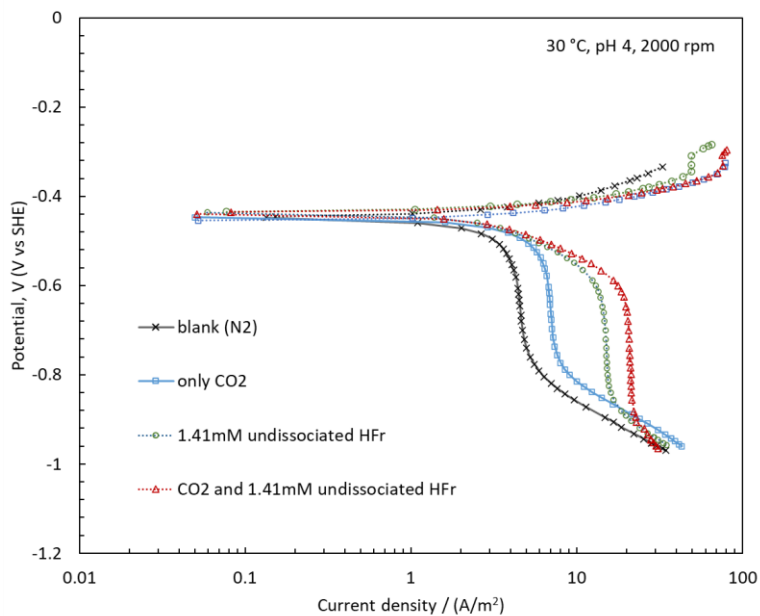
Effect of HFr on CO₂ corrosion

Similar electrochemical experiments were performed in CO₂ sparged electrolyte at different concentrations, temperature, and pH. The details of the experimental parameters are listed in Table 5.

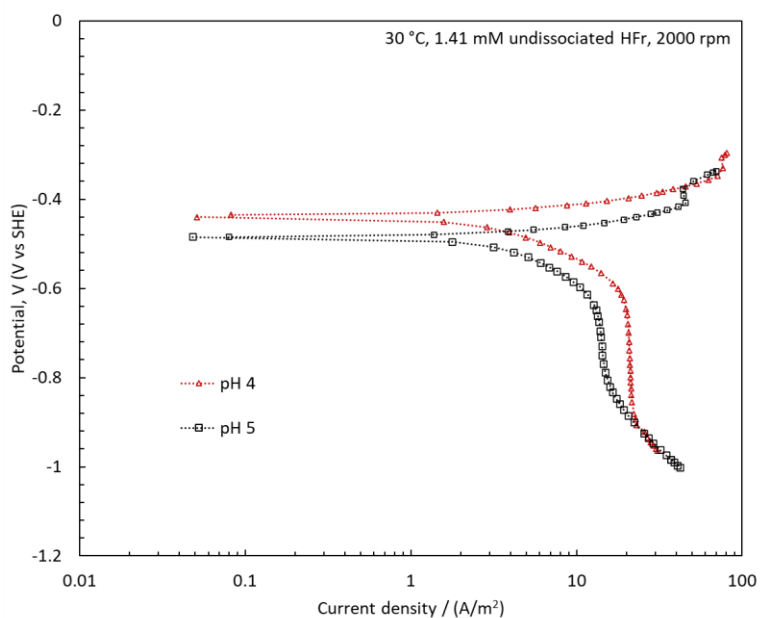
**Table 5
Parameters for experiments conducted in a CO₂ sparged solution**

Parameter	HFr concentration		Effect of pH		Effect of temperature	
Electrolyte	1 wt% NaCl		1 wt% NaCl		1 wt% NaCl	
RDE rotation speed (rpm)	2000		2000		2000	
Total HFr (mM)	0	3.91	3.91	26.38	3.91	3.41
Undissociated HFr (mM)	0	1.41	1.41		1.41	
pH	4.00		4	5	4.00	
Temperature (°C)	30 ± 2		30 ± 2		30 ± 2	80 ± 2
pCO ₂ (bar)	0.96		0.96		0.96	0.53

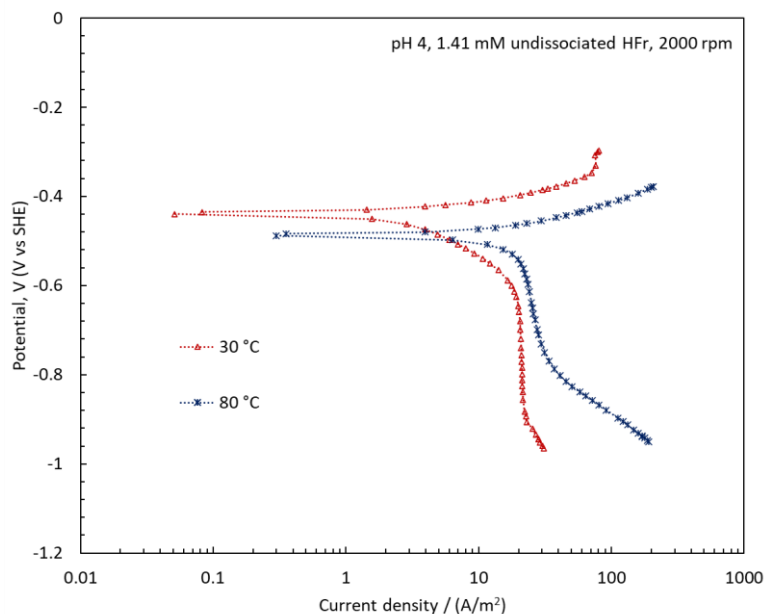
Figure 11 shows the polarization curves obtained from these experiments. As can be seen in Figure 11(a), the aqueous CO₂ environment contributes to the corrosion reaction by dissociation of carbonic acid, which induces buffering effect by replenishing the consumed hydrogen ions. This causes an increase in the limiting current and contributes to an increase in the corrosion rate. In a system containing both HFr and dissolved CO₂, both HFr and H₂CO₃ dissociate and supply H⁺ ions, inducing the buffering effect. The corrosion rates in this scenario are greater than in a system only containing HFr species. The increase in pH as shown in Figure 11(b) causes opposing effects on the cathodic reaction rate (decrease) and anodic reaction rate (increase), as was observed in the case of a system containing only HFr species. This causes a slight decrease in the corrosion rate. The results clearly indicate an increase in the anodic reaction rate and change in the reaction mechanism with increase in pH. As stated earlier, the effect of HFr on this phenomenon is yet to be explored and will be a part of a future study. Lastly, with increase in temperature, a dramatic increase in corrosion rate can be observed in Figure 11(c). This is because the reaction changes from a charge transfer controlled mechanism to a mass transfer-controlled mechanism. Corrosion rates for different experimental conditions are shown in Figure 12.



11(a) Effect of addition of weak acids



11(b) Effect of pH



11(c) Effect of temperature

Figure 11: Polarization curves for X65 steel RDE under different experimental conditions in a CO₂ sparged solution

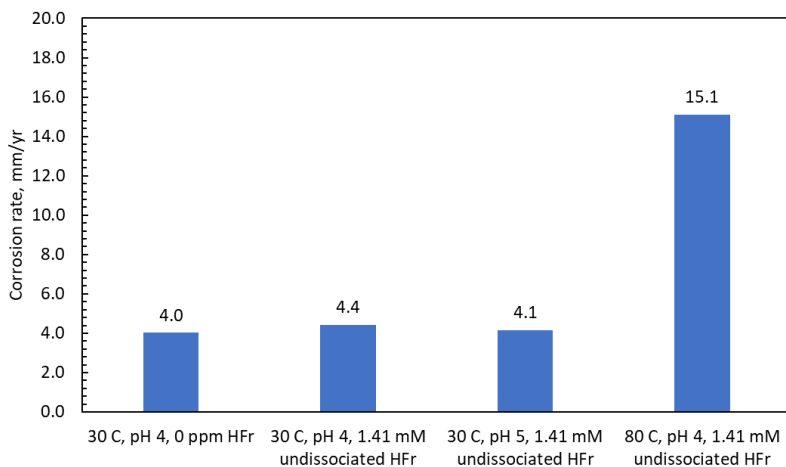


Figure 12: Corrosion rates of X65 steel RDE in CO₂ sparged solution

Comparison of the effect of HFr and HAc on corrosion of mild steel

Fajardo et al.¹¹ performed an electrochemical study to determine the effect of different organic acids (formic acid, acetic acid, and propionic acid) on CO₂ corrosion of mild steel. They performed the polarization studies on a rotating cylindrical electrode made of API 5L X65 steel under non-scaling conditions: pH4, 25 °C, 1000rpm, 0.96 bar of CO₂. They observed that at the same pH and concentration of undissociated organic acids, there was no significant difference in the electrochemical behavior of different organic acids.¹¹ However, these limited number of experiments were conducted in a CO₂ environment, and comparisons were made between the same concentrations of undissociated organic acids measured in ppm instead of molarity. These limitations are addressed in the present study.

Hypothesis 1: The influence of HFr on cathodic and anodic reactions is same as that of HAc.

In order to test this hypothesis, results of electrochemical experiments conducted with the same concentrations of undissociated HFr and HAc were compared. The experimental parameters are listed in Table 6. Polarization curves obtained from these experiments are shown in Figure 13.

Table 6
Experimental parameters used to test Hypothesis 1

Parameter	Effect of HAc concentration				Effect of HFr concentration			
Electrolyte	1 wt% NaCl				1 wt% NaCl			
RDE rotation speed (rpm)	2000				2000			
Total Organic Acid (mM)	0	0.167	1.67	16.7	0	0.39	3.91	39.1
Undissociated Organic Acid(mM)	0	0.14	1.41	14.1	0	0.14	1.41	14.1
pH	4.00 ± 0.02				4.00 ± 0.02			
Temperature (°C)	30 ± 2				30 ± 2			
Sparge gas	N ₂				N ₂			

The results for both HFr and HAc clearly indicate that the increase in the concentration of undissociated acid primarily results in an increase in the limiting current but does not influence the Tafel slope associated with the charge transfer reaction. Furthermore, the limiting current values in test solutions containing the same concentrations of undissociated HFr and HAc are almost same (dotted lines in Figure 13). This implies that the hypothesis tests 'True' for cathodic reactions. i.e., HFr and HAc have a similar effect on the cathodic reaction.

However, the hypothesis tests 'False' for the anodic reaction. While HAc is observed to slightly retard the anodic reaction, resulting in a decrease in corrosion rate with increasing concentration, the same is not true for HFr. The retardation of the anodic (iron dissolution) reaction in the presence of HAc has been reported by multiple authors.^{4, 12-14} The effect of HAc on anodic curves is also reflected in the slight shift in corrosion potential values. No such behavior is observed in the case of HFr. As there is no influence of HFr on the anodic reaction, the corrosion rate continues to increase with increasing concentration. A comparison of corrosion rates is shown in Figure 14. HAc is clearly less corrosive than HFr at higher concentrations of undissociated acid due to the retardation of the anodic reaction by HAc.

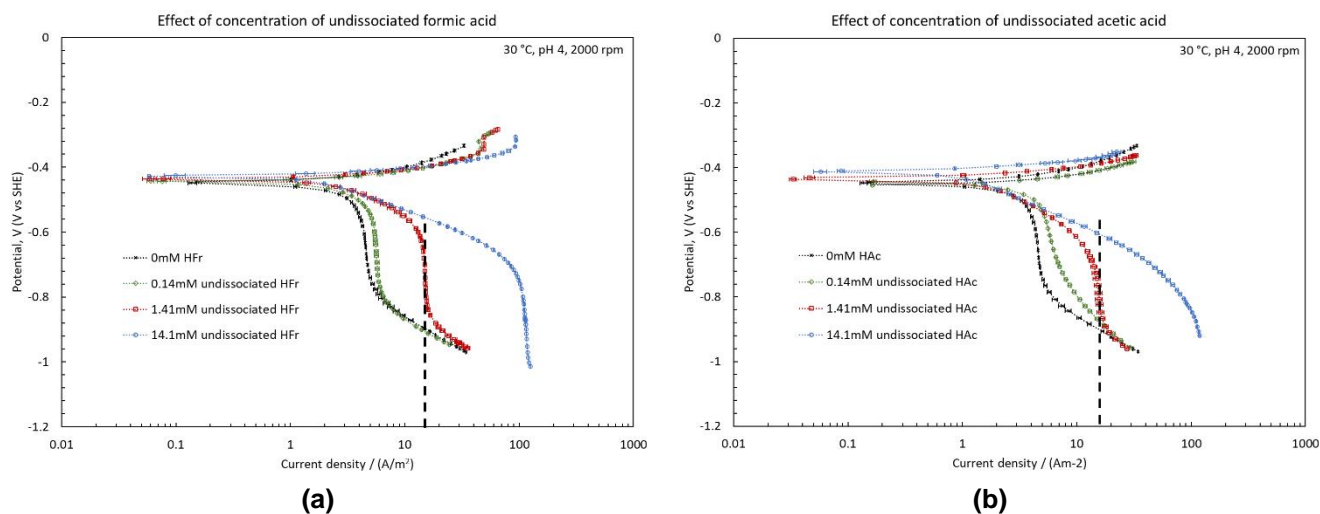


Figure 13: Polarization curves for X65 steel RDE at 30°C, pH 4, 2000 rpm in N₂ sparged, 1 wt% NaCl solution with different concentrations of (a) HFr (b) HAc

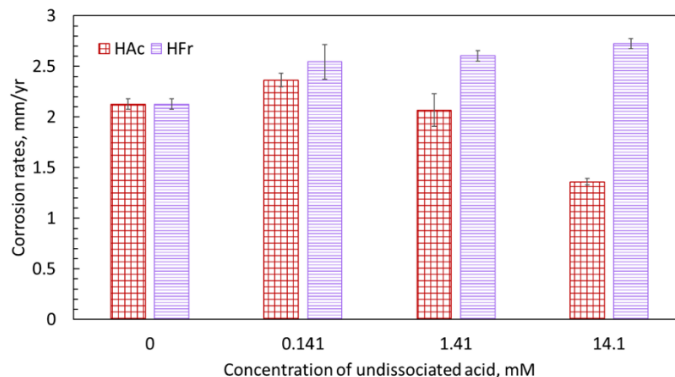


Figure 14: Corrosion rates of X65 steel RDE at 30°C, pH 4, 2000 rpm in N₂ sparged, 1 wt% NaCl solution with different concentrations of HFr and HAC

Hypothesis 2: Under the same experimental conditions (concentrations of undissociated acid, pH, temperature, and flowrate), HFr is always more corrosive than HAC.

In order to test the current hypothesis, results of electrochemical experiments conducted at different temperatures with 1.41 mM of undissociated HFr and HAC were compared. The experimental parameters are listed in Table 7. Polarization curves obtained from these experiments are shown in Figure 15.

**Table 7
Experimental parameters used to test Hypothesis 2**

Parameter	Effect of HAC concentration			Effect of HFr concentration		
Electrolyte	1 wt% NaCl			1 wt% NaCl		
RDE rotation speed (rpm)	2000			2000		
Total Organic Acid (mM)	1.67	1.63	1.61	3.91	3.82	3.41
Undissociated Organic Acid (mM)	1.41			1.41		
pH	4.00			4.00		
Temperature (°C)	30	50	80	30	50	80
Sparge gas	N ₂			N ₂		

The polarization curves for HAC are represented as solid lines and those for HFr by dashed lines in Figure 15. The results indicate that at 30°C, limiting current densities of HAC and HFr are approximately the same. However, with increasing temperature, the limiting current for HFr is significantly lower than that for HAC. This behavior is clearly reflected in the corrosion rate values shown in Figure 16 as the reaction mechanism transforms from a primarily charge transfer controlled process to a primarily mass transfer controlled process. Although HFr is more corrosive at 30°C, the corrosivity of HAC increases as temperature increases. These results appear to be counter-intuitive based on the dissociation constants of HAC (pKa=4.86) and HFr (pKa=3.85) at 80°C. There is a need for further investigation to verify the results. As per the current experimental results, the hypothesis tests 'False', i.e., the corrosivity of HAC vs HFr is dependent on temperature.

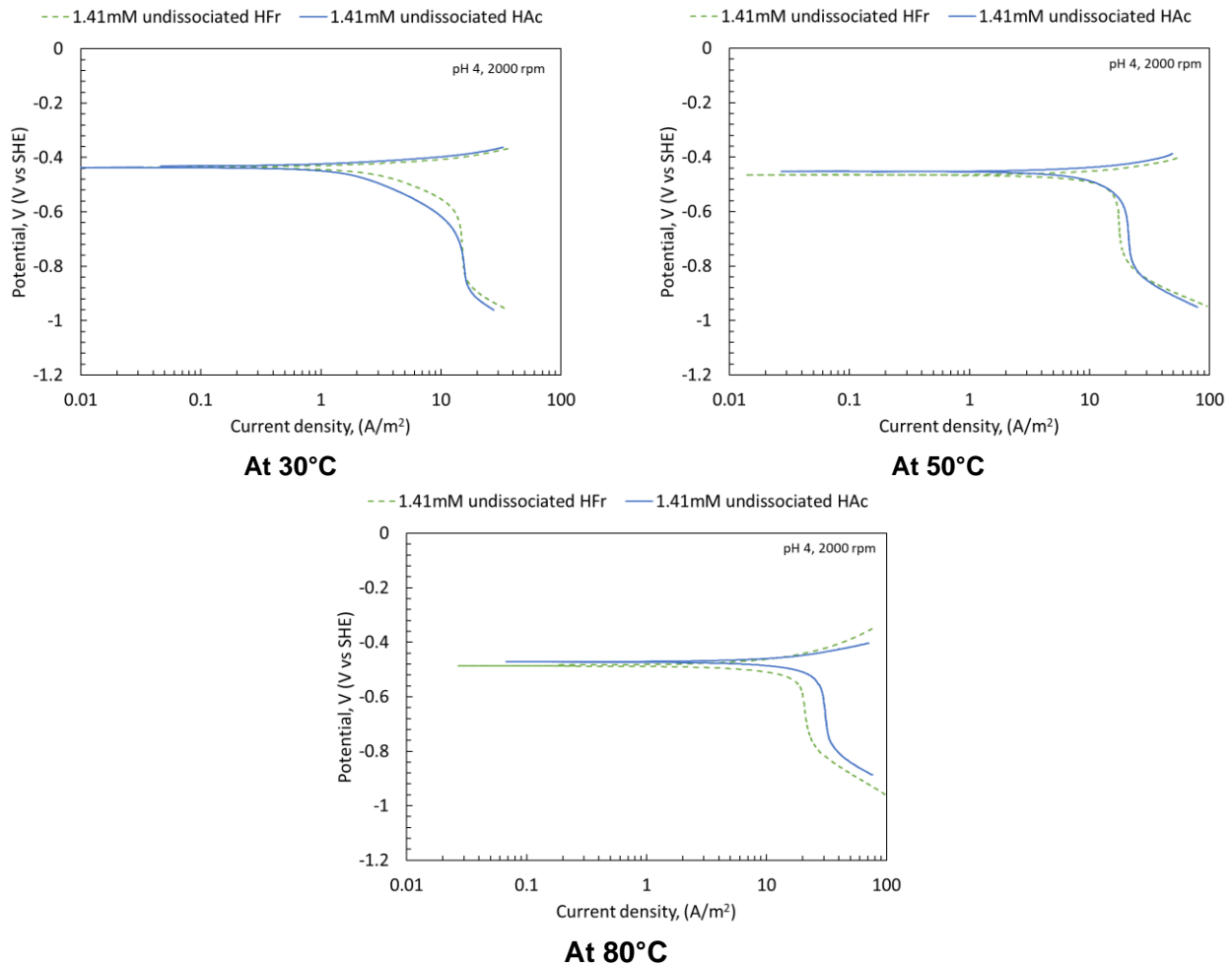


Figure 15: Polarization curves for X65 steel RDE at pH 4, 2000 rpm, 1.41 mM undissociated organic acid (HAc or HFr) in N₂ sparged, 1 wt% NaCl solution.

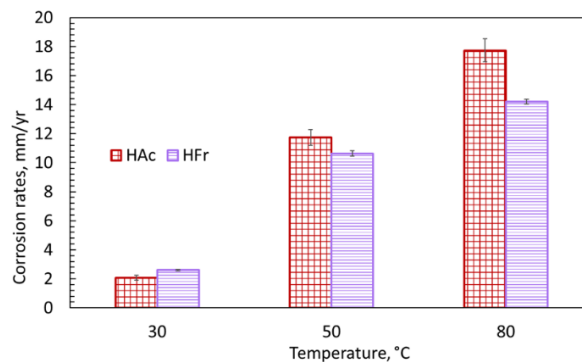


Figure 16: Corrosion rates of X65 steel RDE at pH 4, 2000 rpm, 1.41 mM undissociated organic acid (HAc or HFr) in N₂ sparged, 1 wt% NaCl solution at 30, 50, & 80°C.

CONCLUSIONS

1. In the presence of HFr, the hydrogen evolution reaction is the main cathodic reaction affecting the corrosion of mild steel.
2. The contribution of HFr to the corrosion process is through its chemical dissociation, which induces the buffering effect by replenishing H⁺ ions. This contributes to the increase in limiting current density with increase in concentration of HFr.

3. In the presence of HFr, the anodic reaction rate and reaction mechanism were observed to change with increase in pH.
4. While HAc was observed to slightly retard the anodic reaction, resulting in a decrease in corrosion rate with increasing concentration, the same was not true for HFr. Consequently, with increase in concentration of undissociated organic acid at 30 °C, corrosion rates decreased with an increase in HAc concentration while they increased with a similar increase in HFr concentration.
5. Although HFr was more corrosive than HAc at 30 °C, it was observed that HAc was more corrosive than HFr at both 50°C and 80°C. There is a need for further investigation focusing on the adsorption kinetics of HAc and HFr at different temperatures.

ACKNOWLEDGEMENTS

The author would like to thank the following companies for their financial support:

Ansys, Baker Hughes, BP, Chevron, Clariant Corporation, CNOOC, ConocoPhillips, M-I SWACO (Schlumberger), Multi-Chem (Halliburton), Occidental Oil Company, Pertamina, Saudi Aramco, Shell Global Solutions, Sinclair Energy Partners, SINOPEC (China Petroleum), and TOTAL.

REFERENCES

- [1] C. De Waard and D. E. Milliams, "Carbonic acid corrosion of steel.," *Corrosion*, Vol. 31, No. 5. pp. 177–181, 1975.
- [2] M. R. Bonis and J. L. Crolet, "Prediction of the risks of CO₂ corrosion in oil and gas wells," *SPE Prod. Facil.*, Vol. 6, No. 4, pp. 449–453, 1991.
- [3] M. Bonis and J. L. Crolet, "The role of acetate ions in CO₂ corrosion," *CORROSION conf.*, No.160, pp. 281–294, 1983.
- [4] J. L. Crolet, N. Thevenot, and A. Dugstad, "Role of free acetic acid on the CO₂ corrosion of steels," *CORROSION conf.*, No. 24, pp. 1–16, 1999.
- [5] B. R. Linter and G. T. Burstein, "Reactions of pipeline steels in carbon dioxide solutions," *Corros. Sci.*, Vol. 41, No. 1, pp. 117–139, 1999.
- [6] J. Amri, E. Gulbrandsen, and R. P. Nogueira, "Numerical simulation of a single corrosion pit in CO₂ and acetic acid environments," *Corros. Sci.*, Vol. 52, No. 5, pp. 1728–1737, 2010.
- [7] A. Kahyarian and S. Nestic, "A new narrative for CO₂ corrosion of mild steel," *J. Electrochem. Soc.*, Vol. 166, No. 11, pp. C3048–C3063, 2019.
- [8] R. H. Perry and D. Green, *Perry's chemical engineers' handbook*, 7th ed. McGraw Hill, 1997.
- [9] G. F. A. Kortüm, W. Vogel, and K. Andrussow, *Dissociation constants of organic acids in aqueous solution*. London: Butterworths, 1961.
- [10] S. Nestic, N. Thevenot, J. L. Crolet, and D. Drazic, "Electrochemical properties of iron dissolution in the presence of CO₂ - Basics revisited," *CORROSION conf.*, No. 003, pp. 1 - 23, 1996.
- [11] V. Fajardo, C. Canto, B. Brown, and S. Nestic, "Effect of organic acids in CO₂ corrosion," *CORROSION conf.*, No. 319, pp. 1–18, 2007.
- [12] E. Gulbrandsen and K. Bilkova, "Solution chemistry effects on corrosion of carbon steels in presence of CO₂ and acetic acid," *CORROSION conf.*, No. 364, pp. 1–37, 2006.
- [13] J. Amri, E. Gulbrandsen, and R. P. Nogueira, "Role of acetic acid in CO₂ top of the line corrosion of carbon steel," *CORROSION conf.*, No. 11329, pp. 1 - 22, 2011.
- [14] A. Kahyarian, B. Brown, and S. Nešić, "Mechanism of cathodic reactions in acetic acid corrosion of iron and mild steel," *Corrosion*, Vol. 72, No. 12, pp. 1539–1546, 2016.